The Astrophysical Journal, 661:650–659, 2007 June 1

THE VELOCITY FIELD OF THE LOCAL UNIVERSE FROM MEASUREMENTS OF TYPE Ia SUPERNOVAE

Troels Haugbølle,[1] Steen Hannestad,[1] Bjarne Thomsen,[1] Johan Fynbo,[2] Jesper Sollerman,[2] and Saurabh Jha[3]

Received 2006 December 7; accepted 2007 February 1

ABSTRACT

We present a measurement of the velocity flow of the local universe relative to the CMB rest frame, based on the recent Jha et al. sample of 133 low-redshift Type Ia supernovae. At a depth of 4500 km s^{-1} we find a dipole amplitude of 279 ± 68 km s^{-1} in the direction $l = 285^\circ \pm 18^\circ$, $b = -10^\circ \pm 15^\circ$, consistent with earlier measurements and with the assumption that the local velocity field is dominated by the Great Attractor region. At a greater depth of 5900 km s^{-1}, we find a shift in the dipole direction toward the Shapley Concentration. We also present the first measurement of the quadrupole term in the local velocity flow at these depths. Finally, we have performed detailed studies based on *N*-body simulations of the expected precision with which the lowest multipoles in the velocity field can be measured out to redshifts of order 0.1. Our mock catalogs are in good agreement with current observations and demonstrate that our results are robust with respect to assumptions about the influence of local environment on the Type Ia supernova rate.

Subject headings: galaxies: distances and redshifts — galaxies: statistics — large-scale structure of universe — supernovae: general

Online material: color figures

1. INTRODUCTION

Distant Type Ia supernovae (SNe Ia) have been used to probe the expansion rate of the universe out to redshifts of order 1.5 (see, e.g., Riess et al. 2004). These measurements were crucial in establishing the current standard model of cosmology, in which roughly 30% of the energy density is in the form of nonrelativistic matter whereas roughly 70% is in the form of a dark energy, a component with negative pressure.

The power of supernova surveys as cosmological probes depends on precise measurement of the luminosity distances to the individual supernovae—but the supernova host galaxies do not follow the Hubble flow. They have peculiar velocities, induced by the underlying gravitational potential, and the measured luminosity distances and redshifts are perturbed in correlation with the large-scale structure (see, e.g., Miller & Branch 1992).

The measured fluctuations in the luminosity distances from surveys of nearby supernovae can be related to the local variation in the Hubble parameter (Riess et al. 1995) and the local large-scale structure, and they can be quantified in terms of their correlation functions. This possibility has been studied in several recent papers (Bonvin et al. 2006a, 2006b; Hui & Greene 2006; see also Sugiura et al. 1999) using analytical methods. Bonvin et al. (2006b) detected the dipole term with respect to the cosmic microwave background (CMB) at roughly 2 σ confidence. The variation of the monopole contribution with redshift was studied by Zehavi et al. (1998) using the same supernova sample as Riess et al. (1995).

In contrast to measurements of the density field, velocity field measurements are much less sensitive to selection bias, since the field is measured directly instead of being summed up from number counting, but it is very sensitive to uncertainties in the measured luminosity distance. Because of this, SNe Ia are particularly useful as probes of the velocity field, thanks to the very small inherent uncertainty in their luminosity distance. Compared with measurements using galaxies as standard candles, much fewer supernovae are needed in order to obtain a reliable estimate of at least the lowest multipoles in the velocity field.

The purpose of the present paper is twofold. The first is to perform a theoretical study of the problem of extracting the velocity field from supernova data. The second is to use the developed formalism on the best available data set to extract precise values of the dipole and quadrupole terms in the local velocity field.

We first use large-scale dark matter *N*-body models to predict the observed angular power spectrum of the peculiar radial velocity field as a function of redshift and to explore its utility as a probe of the local velocity field. By using this method, we are able to quantify the effect of various error sources as well as cosmic variance.

We also use the Jha et al. (2007) sample (hereafter the JRK sample) of nearby SNe Ia to calculate the lowest multipoles of the local velocity field. We find that both the dipole and the quadrupole terms are well measured by this sample. Higher multipoles cannot be reliably estimated with the JRK sample because of sparse sampling. In Jha et al. (2007) this sample was also used to probe the monopole term in an analysis similar to that of Zehavi et al. (1998). Similar evidence of a local void was found, even taking a data set that is completely disjoint from that of Zehavi et al. In the following, we concentrate on the dipole and quadrupole terms in the JRK sample, since the monopole has already been exhaustively discussed in Jha et al. (2007).

In § 2, we discuss the formalism used to derive the velocity field from magnitude measurements. In § 3, we present the analysis tools used to extract the multipole components of the velocity field from a finite sample of supernovae. In § 4, we use catalogs from *N*-body simulations to study the expected properties of the velocity field, including the precision with which it can be probed by supernova surveys. We apply the same

[1] Department of Physics and Astronomy, University of Aarhus, DK-8000 Aarhus C, Denmark; haugboel@phys.au.dk.

[2] Dark Cosmology Centre, Niels Bohr Institute, University of Copenhagen, DK-2100 Copenhagen Ø, Denmark.

[3] Kavli Institute for Particle Astrophysics and Cosmology, Stanford Linear Accelerator Center, Menlo Park, CA 94025.

formalism to the JRK sample and provide a detailed discussion of the results in § 5. Finally, § 6 contains a comparison with other measurements of the local velocity field, and in § 7 we provide our conclusions. In the following, we take $c = 1$.

2. DISTANCE MEASURES AND RADIAL VELOCITIES

The luminosity distance, d_L, to a supernova at redshift z is defined by

$$d_L = \sqrt{\frac{L}{4\pi F}}, \tag{1}$$

where F is the observed flux and L is the luminosity, or, equivalently, by

$$m = 5 \log \left(\frac{d_L}{1 \text{ Mpc}} \right) + M + 25, \tag{2}$$

where m is the apparent and M is the absolute magnitude. The angular diameter distance, d_A, to the same supernova is defined as

$$d_A = \frac{d_L}{(1+z)^2}. \tag{3}$$

In a homogeneous and isotropic universe, the two distance measures, d_L and d_A, are given by

$$d_A(1+z) = \frac{d_L}{1+z} = \frac{1}{H_0} \begin{cases} \frac{1}{\sqrt{\Omega - 1}} \sin(\sqrt{\Omega - 1} I), & \text{if } \Omega > 1, \\ I, & \text{if } \Omega = 1, \\ \frac{1}{\sqrt{1 - \Omega}} \sinh(\sqrt{1 - \Omega} I), & \text{if } \Omega < 1, \end{cases} \tag{4}$$

where

$$I = H_0 \int_0^z \frac{dz}{H(z)} = \int_1^{1+z} \frac{dx}{\sqrt{\Omega_m x^3 + \Omega_K x^2 + \Omega_\Lambda}}. \tag{5}$$

By taking the logarithmic derivative of equation (4) with respect to $1 + z$ in the special case of a flat universe ($\Omega = 1$), we obtain

$$\alpha_L(z) - 1 = \alpha_A(z) + 1 = \frac{1}{H(z) d_A(z)} = \frac{(1+z)^2}{H(z) d_L(z)}, \tag{6}$$

where

$$\alpha_L = \frac{d \ln d_L}{d \ln (1+z)}, \quad \alpha_A = \frac{d \ln d_A}{d \ln (1+z)}. \tag{7}$$

However, in a perturbed universe the luminosity distance depends on the detailed trajectory of the individual photons from the supernova to the observer. At moderately high redshifts ($z \gtrsim 0.5$), the contribution arising from lensing by intervening matter dominates, while at low redshifts ($z \lesssim 0.5$) the contribution from the peculiar velocities of the supernova host galaxies relative to the observer dominates. In this paper we are only concerned with the local universe. From now on, we will therefore only consider the contribution from the peculiar velocities in determining distances. For a given supernova and observer, each with some peculiar velocity, the measured redshift z, angular diameter distance d_A, and luminosity distance d_L are modified according to

$$1 + z = (1 - \boldsymbol{v}_0 \cdot \boldsymbol{n})(1 + \bar{z})(1 + v_r), \tag{8}$$

$$d_A = \bar{d}_A(\bar{z})(1 + \boldsymbol{v}_0 \cdot \boldsymbol{n}), \tag{9}$$

$$d_L = \bar{d}_L(\bar{z})(1 + \boldsymbol{v}_0 \cdot \boldsymbol{n})(1 + v_r - \boldsymbol{v}_0 \cdot \boldsymbol{n})^2 \tag{10}$$

(Hui & Greene 2006; Bonvin et al. 2006b), where by definition

$$d_L \equiv d_A(1+z)^2, \quad \bar{d}_L(\bar{z}) \equiv \bar{d}_A(\bar{z})(1+\bar{z})^2. \tag{11}$$

Overbars indicate quantities as measured in a homogeneous and isotropic cosmology, and $v_r = \boldsymbol{v}_e \cdot \boldsymbol{n}$ is the velocity of the supernova projected along the direction from the observer to the supernova. Having measured the redshift z and the flux F of the supernova, we can calculate the luminosity distance d_L and the angular diameter distance d_A to within a scatter determined by the cosmic variance on its luminosity, L. As we know the peculiar velocity, $\boldsymbol{v}_0$, of the observer with respect to the CMB with great accuracy, it is useful to collect all known quantities on the left-hand side of the three equations:

$$1 + \hat{z} = (1+z)(1 + \boldsymbol{v}_0 \cdot \boldsymbol{n}) = (1+\bar{z})(1+v_r), \tag{12}$$

$$\hat{d}_A = d_A(1 - \boldsymbol{v}_0 \cdot \boldsymbol{n}) = \bar{d}_A(\bar{z}), \tag{13}$$

$$\hat{d}_L = d_L(1 + \boldsymbol{v}_0 \cdot \boldsymbol{n}) = \bar{d}_L(\bar{z})(1 + 2v_r). \tag{14}$$

The three quantities $\hat{z}$, $\hat{d}_A$, and $\hat{d}_L$ are the redshift, angular diameter distance, and luminosity distance as measured and calculated by an observer at rest with respect to the CMB. In the following we assume that the measured quantities all have been corrected to a frame at rest with respect to the CMB. The measured redshift, $\hat{z}$, is most transparently split into the cosmological redshift, $\bar{z}$, and the radial velocity of the supernova, v_r, by inverting equation (13) to find $\bar{z}$, which is then inserted into this alternative form of equation (12):

$$v_r = \ln(1+\hat{z}) - \ln(1+\bar{z}). \tag{15}$$

It is also possible to begin with equation (15) to obtain the cosmological redshift, $\bar{z}$, in terms of the measured redshift $\hat{z}$ and the radial velocity v_r of the supernova:

$$\ln(1+\bar{z}) = \ln(1+\hat{z}) - v_r. \tag{16}$$

We now expand the natural logarithm of the angular diameter distance, $\ln \bar{d}_A(\bar{z})$, to first order around the measured redshift $\hat{z}$, and by using equation (13) we obtain

$$\ln \hat{d}_A = \ln \bar{d}_A(\bar{z}) = \ln \bar{d}_A(\hat{z}) - \alpha_A(\hat{z}) v_r, \tag{17}$$

where $\alpha_A(z)$ for a flat universe is given by equation (6). This equation applies equally well for the luminosity distance, so we can give a common formula for both distance measures:

$$\ln \left[\frac{\hat{d}_L}{\bar{d}_L(\hat{z})} \right] = \ln \left[\frac{\hat{d}_A}{\bar{d}_A(\hat{z})} \right] = -\alpha_A(\hat{z}) v_r. \tag{18}$$

This expression can easily be transformed into an equation between the measured apparent magnitude, $\hat{m}$, the calculated

apparent magnitude, $\bar{m}(\hat{z})$, at the measured redshift, $\hat{z}$, and the peculiar radial velocity, v_r, of the supernova:

$$\hat{m} - \bar{m}(\hat{z}) = 5 \log \left[\frac{\hat{d}_L}{\bar{d}_L(\hat{z})} \right] = - \frac{5}{\ln 10} \alpha_A(\hat{z}) v_r. \quad (19)$$

Inverting this equation for the special case of a flat universe, we obtain

$$v_r = - \frac{\ln 10}{5} \left[\frac{H(\hat{z}) \bar{d}_A(\hat{z})}{1 - H(\hat{z}) \bar{d}_A(\hat{z})} \right] [\hat{m} - \bar{m}(\hat{z})]. \quad (20)$$

For low-redshift supernovae, the Hubble parameter, the angular diameter distance, and the luminosity distance can all be expanded in terms of the deceleration parameter, q_0:

$$H(z) = H_0[1 + (1 + q_0)z], \quad (21)$$

$$\bar{d}_A(z) = \frac{z}{H_0}[1 - (3 + q_0)z/2], \quad (22)$$

$$\bar{d}_L(z) = \frac{z}{H_0}[1 + (1 - q_0)z/2]. \quad (23)$$

When we insert these values into equation (20), we obtain the radial velocity of a low-redshift supernova,

$$v_r = -(\ln 10/5)\hat{z}[1 + (1 + q_0)\hat{z}/2][\hat{m} - \bar{m}(\hat{z})]. \quad (24)$$

In this approximation the distance modulus, $m - M$, is given by

$$\bar{m}(\hat{z}) - M = 42.3841 - 5 \log h + 5 \log \hat{z} + (2.5/\ln 10)(1 - q_0)\hat{z}, \quad (25)$$

where the Hubble constant as usual is given as $H_0 = 100\ h$ km s^{-1} Mpc^{-1}. The distance modulus defined in equation (25) should be compared with the distance modulus $\hat{m} - M$ as measured in a frame at rest with respect to the CMB. The difference between the apparent magnitude $\hat{m}$ and that measured by the observer, m, is, according to equation (14),

$$\hat{m} - m = (5/\ln 10)\boldsymbol{v}_0 \cdot \boldsymbol{n} = 2.17 \boldsymbol{v}_0 \cdot \boldsymbol{n}. \quad (26)$$

The approximate equation (24) is sufficient for the low redshifts that we are considering, while at higher redshifts one has to use the correct form, equation (20), and also take into account other contributions to $\hat{m} - \bar{m}(\hat{z})$, such as lensing.

3. ANALYSIS USING AN ANGULAR EXPANSION OF THE RADIAL VELOCITY FIELD

We analyze both the mock catalogs discussed in the next section and the real data set (see § 5) using the same technique. In practice, we decompose the field into spherical harmonics.

The radial velocity is a real scalar field, and on a spherical shell of a given redshift it can be decomposed into spherical harmonics,

$$v_r = \sum_{\ell=0}^{\infty} \sum_{m=-\ell}^{\ell} a_{\ell m} Y_{\ell m} = \sum_{\ell=0}^{\infty} \left[\sum_{m=1}^{\ell} (a_{\ell,-m} Y_{\ell,-m} + a_{\ell m} Y_{\ell m}) + a_{\ell 0} Y_{\ell 0} \right]. \quad (27)$$

Using $a_{\ell,-m} = (-1)^m a^*_{\ell m}$ for the expansion of a real function and $Y_{\ell,-m} = (-1)^m Y^*_{\ell m}$, we obtain

$$v_r = \sum_{\ell=0}^{\infty} \left\{ \sum_{m=1}^{\ell} [2\Re(a_{\ell m} Y_{\ell m})] + a_{\ell 0} Y_{\ell 0} \right\} = \sum_{\ell=0}^{\infty} \left\{ \sum_{m=1}^{\ell} [2\Re(a_{\ell m})\Re(Y_{\ell m}) - 2\Im(a_{\ell m})\Im(Y_{\ell m})] + a_{\ell 0} Y_{\ell 0} \right\}. \quad (28)$$

However, this applies strictly only if the field can be measured on the entire sphere. In our case the radial velocity field is measured for a finite number of directions, so we can only hope to determine a finite number of coefficients $a_{\ell m}$ by fitting a truncated multipole expansion by the method of weighted linear least squares using $\{Y_{\ell 0}, [2\Re(Y_{\ell m}), -2\Im(Y_{\ell m})], m = 1, \ldots, \ell\}$ as basis functions. Specifically, we solve the problem by a singular value decomposition.

We follow the procedure of Copi et al. (2006) and represent the ℓth multipole in terms of a scalar, $A^{(\ell)}$, and ℓ unit vectors, $\{\hat{\boldsymbol{v}}^{(\ell,m)}, m = 1, \ldots, \ell\}$:

$$f_l(\theta, \phi) = A^{(\ell)} \left[\prod_{m=1}^{\ell} (\hat{\boldsymbol{v}}^{(\ell,m)} \cdot \hat{\boldsymbol{e}}) - \mathcal{T}_\ell \right], \quad (29)$$

where $\hat{\boldsymbol{e}} = (\sin\theta \cos\phi, \sin\theta \sin\phi, \cos\theta)$ and $\mathcal{T}_\ell$ is the sum of all possible traces of the first term. In this representation the multipole expansion up to and including the quadrupole term takes the following form:

$$v_r(\hat{\boldsymbol{e}}) = A^{(0)} + A^{(1)}(\hat{\boldsymbol{v}}^{(1,1)} \cdot \hat{\boldsymbol{e}}) + A^{(2)} \left[(\hat{\boldsymbol{v}}^{(2,1)} \cdot \hat{\boldsymbol{e}})(\hat{\boldsymbol{v}}^{(2,2)} \cdot \hat{\boldsymbol{e}}) - \tfrac{1}{3}(\hat{\boldsymbol{v}}^{(2,1)} \cdot \hat{\boldsymbol{v}}^{(2,2)}) \right]. \quad (30)$$

Note that $\hat{\boldsymbol{v}}^{(2,1)}$ and $\hat{\boldsymbol{v}}^{(2,2)}$ are "headless" vectors only defining a line, not a direction. Equivalently, they define a plane, but they do not define a rotation in that plane, so the normal to the plane is also headless. By convention we choose as the first vector, $\hat{\boldsymbol{e}}_1$, the one with the largest absolute z-coordinate. We can choose $\hat{\boldsymbol{e}}_1$ to point to the hemisphere near the pole without introducing a negative amplitude $A^{(2)}$ if both $\hat{\boldsymbol{e}}_1$ and $\hat{\boldsymbol{e}}_2$ have their sign changed. Finally, we define the normal to the plane spanned by the two vectors as $\hat{\boldsymbol{e}}_1 \times \hat{\boldsymbol{e}}_2$. This is the *polar quadrupole vector*.

From the $a_{\ell m}$ coefficients, the monopole amplitude can be found as

$$A^{(0)} = a_{00}/\sqrt{4\pi}, \quad (31)$$

and the dipole amplitude and direction can be found as

$$A^{(1)} = (a_{10}^2 + 2|a_{11}|^2)^{1/2}, \quad (32)$$

$$\theta = -\tan^{-1}[\Im(a_{11})/\Re(a_{11})], \quad (33)$$

$$\phi = \cos^{-1}(a_{10}/A^{(1)}). \quad (34)$$

This is the direction of the maximum of the dipole. All the higher order multipole vectors are found by using the program `mpd_decomp` by Copi et al. (2006).

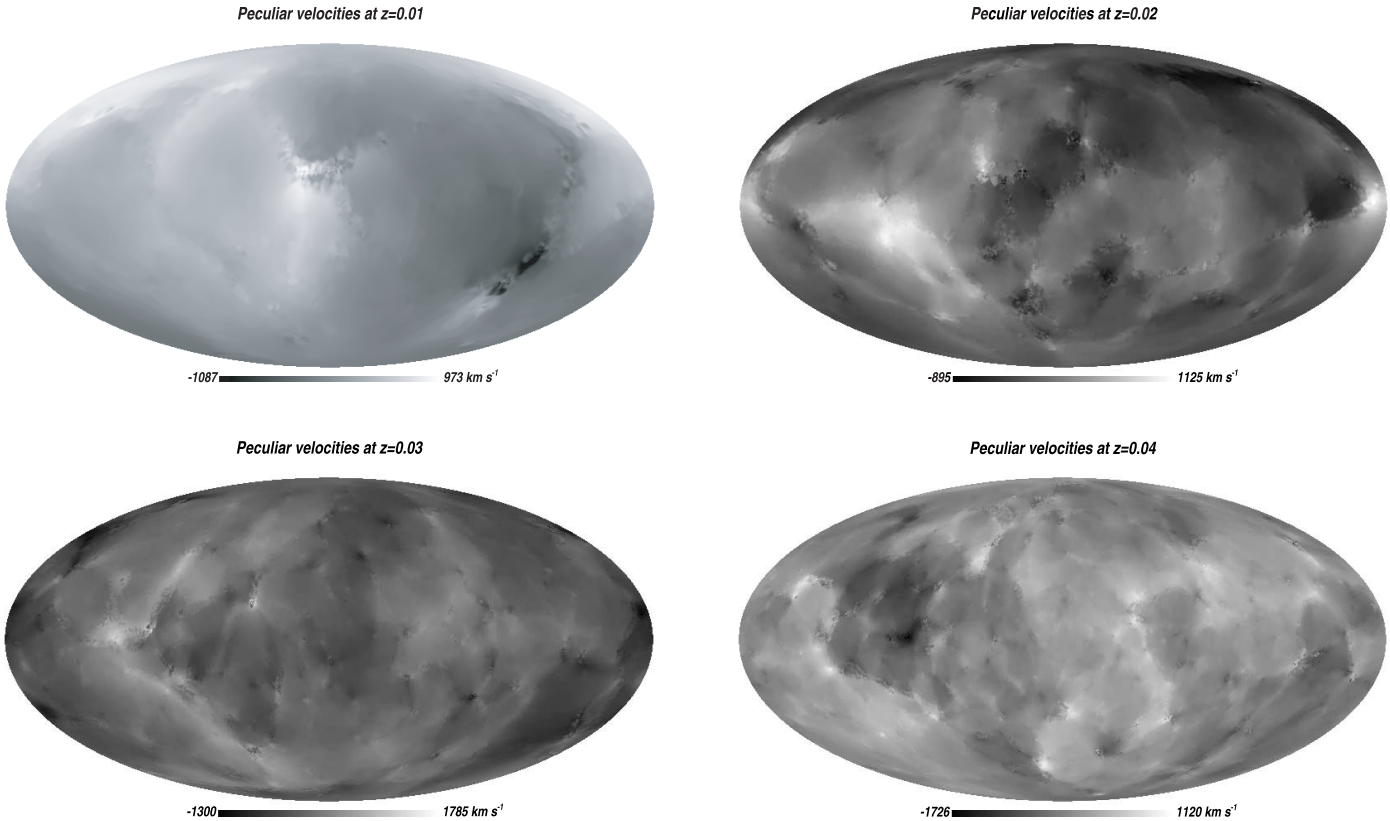

FIG. 1.—Variation in the peculiar velocity at $z = 0.01$–0.04. [*See the electronic edition of the Journal for a color version of this figure*.]

For the lowest ℓ-values, the amplitudes in the multipole vector expansion are related to the usual power C_ℓ as

$$C_0 = 4\pi(A^{(0)})^2, \quad C_1 = \frac{4\pi}{9}(A^{(1)})^2, \tag{35}$$

$$C_2 = \frac{4\pi}{75}(A^{(2)})^2\left[1 + \frac{1}{3}(\hat{\boldsymbol{v}}^{(2,1)} \cdot \hat{\boldsymbol{v}}^{(2,2)})\right] \tag{36}$$

(Copi et al. 2006). It should be noted that in general the individual multipole coefficients obtained in the fit to data can be strongly dependent on the number of modes included. The reason for this is that the window function does not cover the entire sky; rather, there are patches with zero coverage. This means that the spherical harmonics are no longer orthogonal and shows up as a leakage of power between different ℓ's. In fact, this is predicted to be a significant problem for any harmonic analysis with limited sampling, because the higher order multipoles do contribute significantly to the rms velocity. In § 5.1, we discuss the implications of sampling for the JRK sample.

4. SYNTHETIC SUPERNOVA SURVEYS FROM MONTE CARLO SIMULATIONS

Before analyzing existing data, we make mock catalogs of supernova data based on dark matter N-body simulations. This is done in order to obtain an estimate of the various sources of error in such measurements. The N-body simulations were performed with the GADGET-2 code (Springel 2005; Springel et al. 2001) with a box size of 800 h^{-1} Mpc and 512^3 and 768^3 particles, respectively, to make synthetic realizations. The box size is chosen large enough that the periodic nature of the box does not impact the simulation at the scales ($z \lesssim 0.1$, or $\lesssim 300\ h^{-1}$ Mpc) we are interested in, and the high-resolution run is made in order to ensure that our results are not dependent on the numerical resolution. In Figure 1 is shown a typical all-sky map in Mollweide projection of the peculiar velocity field at redshifts $z = 0.01$–0.04, computed in the CMB rest frame.

The formation rate of SNe Ia as a function of the environment is not well known, although there are indications that at low redshifts the rate is directly proportional to the stellar mass and insensitive to the metallicity (Neill et al. 2006; but see Sharon et al. 2007, Sullivan et al. 2006, and references therein for indications of a bimodal distribution). On the other hand, the semi-analytic estimates in the literature (e.g., Bonvin et al. 2006b; Hui & Greene 2006) assume a rate that is uniform on the sky. This is clearly not realistic, but to test the effect on the luminosity distance distributions, we have made synthetic data sets using both a rate proportional to the mass and a uniform distribution. In Figure 2, we show the distribution of peculiar radial velocities in the two models. The differences between the two scenarios are at the few-percent level. Looking at Figure 1, one can see that the radial velocity field is smooth across voids, in contrast to, for example, scalar fields such as the density field. This is because it is only a pseudoscalar, and the underlying vector field can be transported efficiently (i.e., it is easier to change the direction of a vector than to transport a scalar quantity).

4.1. *Making a Mock Supernova Survey*

Real measurements rely on a tracer of the matter distribution, whether it is galaxies or SNe Ia. In any case, only a finite number of objects will be available. Furthermore, there will be a selection bias coming from the presence of Galactic foregrounds, etc. In this work we generate a mock supernova survey using the following strategy:

1. The total number N of measured SNe in a redshift bin is chosen.

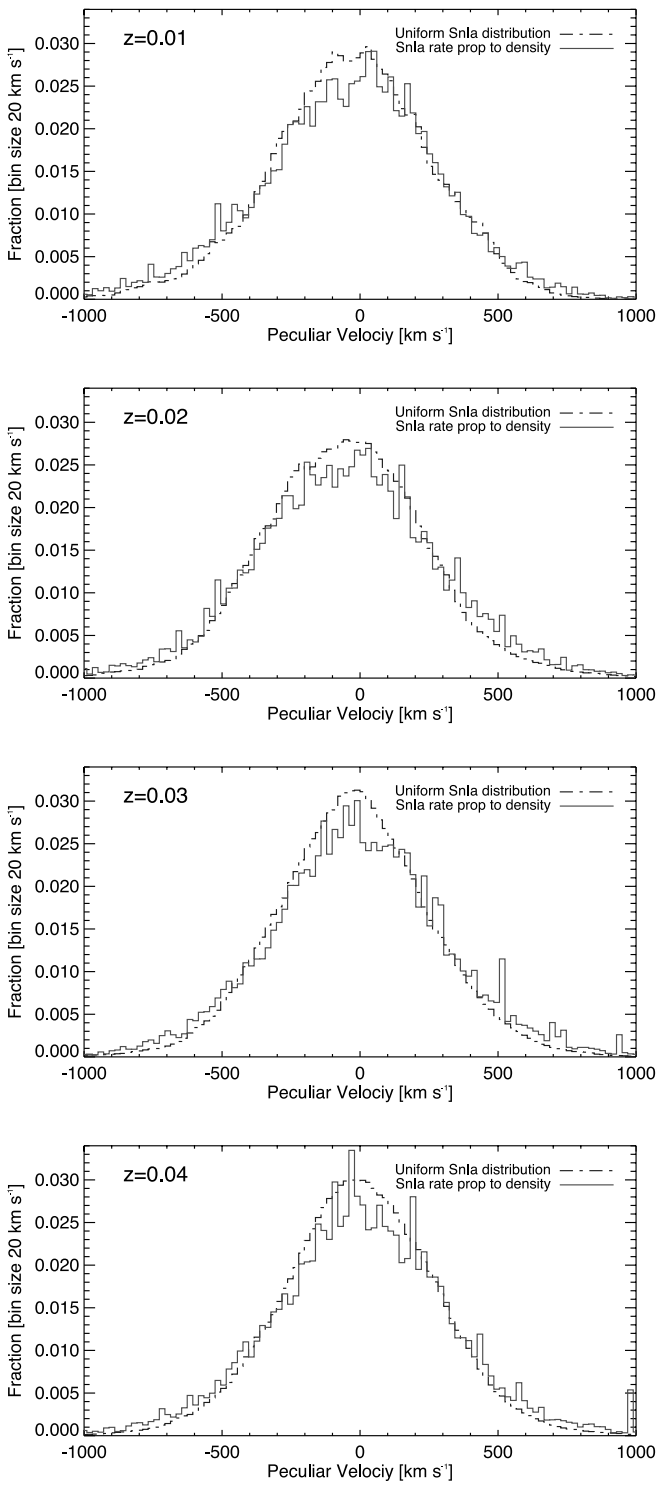

FIG. 2.—Peculiar velocity distribution of supernovae for two different scenarios and at different redshifts. Sampling with an SN Ia rate proportional to the density compared with uniformly on the sky only biases the velocity distribution by a few percent. [*See the electronic edition of the Journal for a color version of this figure.*]

2. Each SN is generated by sampling one of the two probability distributions described in the previous section.

3. To each SN a noise component is added, resulting from scatter in the (stretch-corrected) intrinsic luminosity, uncertainty in extinction correction, measurement errors, etc. We describe the errors as a Gaussian error with a spread of Δm on the measured apparent magnitude of the SN.

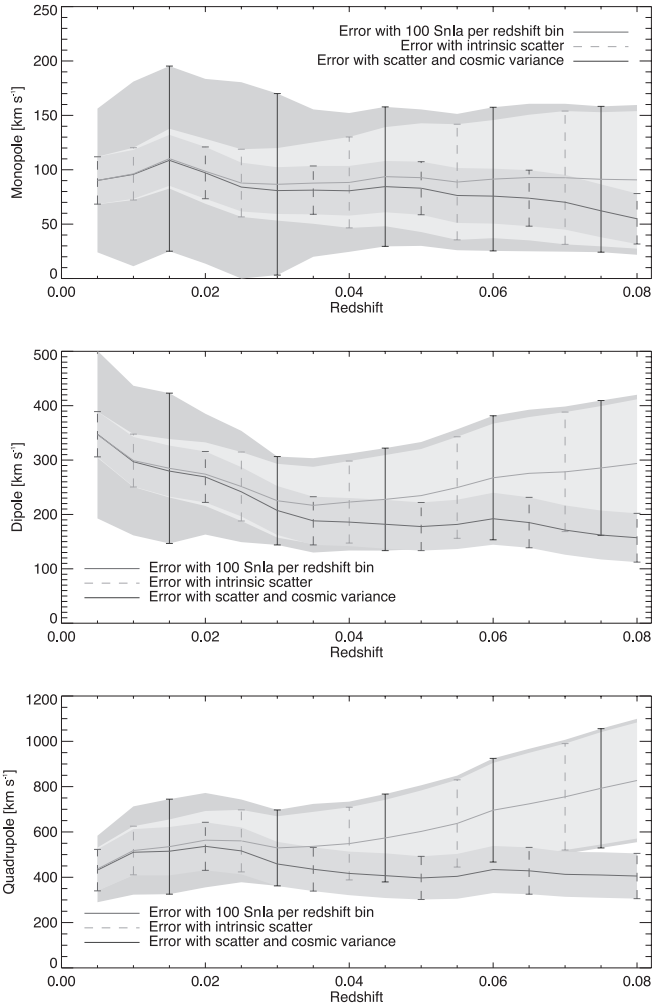

FIG. 3.—Uniform distribution of supernovae: amplitudes of the multipole vectors and the different errors in an SN Ia survey with 100 SNe per redshift bin and an intrinsic scatter in magnitude of $\Delta m = 0.08$. [*See the electronic edition of the Journal for a color version of this figure.*]

From this data set, the angular power spectrum is calculated. For each type of simulated survey, this task is performed 500 times for 27 different observers, to find the mean and variance of the angular power spectrum.

We choose a set of $N = 100$ SNe per bin in 16 redshift bins at redshifts of 0.005–0.08, or equivalently with Hubble flow velocities 1500–24,000 km s^{-1}. This conforms roughly to the expectations from local supernova searches conducted today (Li et al. 2003; Krisciunas et al. 2004; Jha et al. 2006) or in the near future (Aldering et al. 2002; Frieman et al. 2004; Hamuy et al. 2006), if they are divided into three or four redshift bins. In Figures 3–4, we show the evolution of the lowest multipoles as a function of z for both models of the supernova distribution. The black line and error bars show how a hypothetical survey without any external error sources, $\Delta m = 0$, would perform. Hence, the error here is only due to the finite number of SNe that are used to probe the velocity field. The gray line shows the same, but including a Gaussian scatter of $\Delta m = 0.08$. Using the 27 different realizations, we can estimate the size of cosmic variance (*dark gray shaded area*).

From the figures, it is clear that with 100 homogeneous distributed SNe per redshift bin, both the dipole and the quadrupole can be measured out to a redshift of about 0.1. Furthermore, for

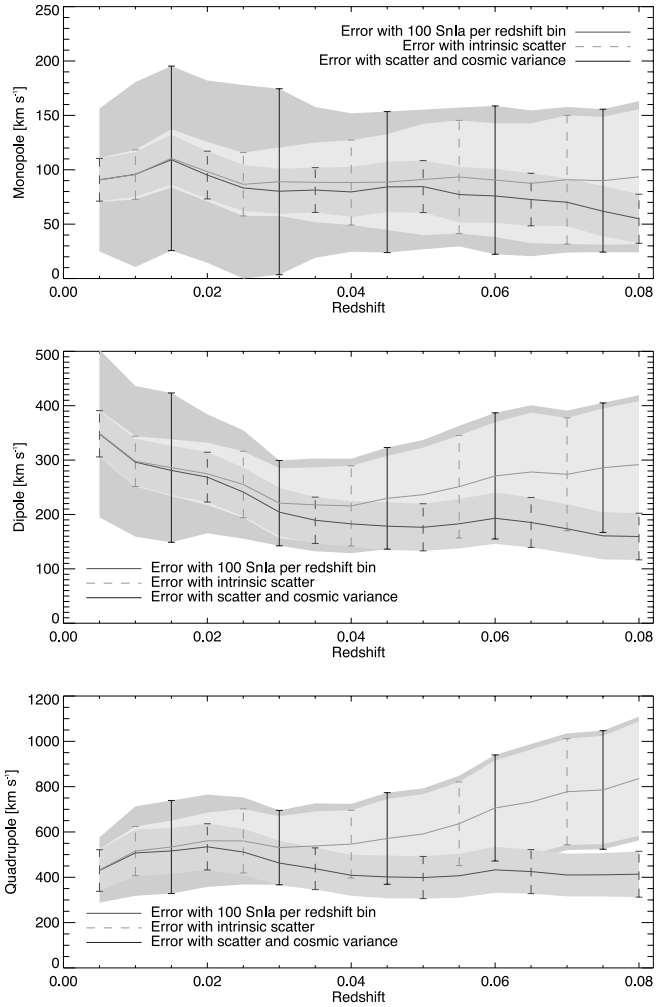

FIG. 4.—Same as Fig. 3, but for a supernova rate proportional to density. [*See the electronic edition of the Journal for a color version of this figure.*]

the synthetic observations we know the underlying cosmology and the real Hubble constant, and we can determine the monopole. In the case of real observations we can only measure the relative change. In other words, the zero point is in principle only measurable asymptotically at high redshifts. Looking at the black curve, one can see that for all multipoles the power goes to zero at higher redshift, as the flow approaches the background Hubble flow. We also note that cosmic variance is very large in the monopole term. This indicates that local "Hubble bubble" phenomena, such as found in Zehavi et al. (1998) and Jha et al. (2007), are not unlikely.

The velocity amplitudes are positive definite, and including a Gaussian scatter in the velocities adds uncorrelated noise to the (synthetic) observations. Therefore, the amplitudes of the multipoles, when errors are included, are overestimated. This error is per se hard to separate from the signal but can trivially be beaten down with better control of the intrinsic errors or by increasing the number of SNe per redshift bin. Given an observational data set, synthetic observations with a realistic sky distribution should be used to separate the noise amplitude from the underlying velocity field.

In accordance with the underlying velocity distribution (Fig. 2), on average there is a 5% overestimation of the radial velocity amplitudes when one assumes the SN Ia rate is proportional to mass, compared with a uniform distribution.

5. RESULTS FROM THE JRK SAMPLE OF NEARBY SUPERNOVAE

We apply the analysis technique described in § 3 to the sample of 133 nearby supernovae obtained by Jha et al. (2007). The JRK sample includes 95 Type Ia supernovae in the Hubble flow, with an intrinsic dispersion of less than 7% in distances. This is the best sample available with distances derived in a homogeneous way, using the multicolor light-curve shape method (MLCS2k2) described in Jha et al. (2007). This method is one of several used to standardize supernova distances, but it is particularly powerful in that it allows a disentangled correction for host galaxy extinction and also provides a statistically reliable way to estimate the errors.

The entire JRK sample comprises 133 supernovae. We have selected three subsamples of these for our analysis. We followed Jha et al. (2007) in selecting as the first subsample 95 Hubble flow supernovae, the *HF sample*, a selection based on distance cut, requirement of an acceptable light-curve fit, and exclusion of objects with very high extinction. The SNe in this sample have redshifts between 0.0085 and 0.021 and a weighted average redshift of $z = 0.0196$, or 5900 km s^{-1}. The second subsample, the *4500 sample*, includes 74 SNe and is similar to the HF sample, but without the highest-redshift SNe and including a few with lower redshift. It has a weighted average of $z = 0.015$, or 4521 km s^{-1}, and contains SNe with redshifts between 0.007 and 0.035. The last subsample, the *3500 sample*, includes 42 SNe and is similar to the 4500 sample, but without the highest-redshift SNe. It has a weighted average of $z = 0.0118$, or 3550 km s^{-1}, and contains SNe with redshifts between 0.007 and 0.017.

To the uncertainties in the distance moduli, we also add in quadrature an additional error of 0.08 mag in order to properly represent the final uncertainties, following Jha et al. (2007). In addition, we add 50 km s^{-1} in quadrature to the errors in the radial velocity in order to take the velocity dispersion around the local anisotropic Hubble flow into account. Karachentsev et al. (2003) find that the radial velocity dispersion around the local (anisotropic) Hubble flow within 5 Mpc amounts to only 41 km s^{-1}, when distance errors are taken into account. For further details on the samples, we refer the reader to Jha et al. (2007).

5.1. *The Effective Window Function*

In Figure 5 we show the distance to the nearest supernova on the sky, measured in degrees, for all points on the sphere. The sample has good coverage, except for a few "holes," mainly defined by the Galactic disk. The mean distance to the nearest supernova is 12.8°, but the maximum distance is 40.5° at $l = 230.4°$, $b = -12.7°$. There are three areas with distance larger than 30°, roughly centered on coordinates (l, b) of (0°, 0°), (80°, −5°), and (230°, −10°), respectively. For a given ℓ, the distance between zero points in the field is $180°/\ell$. If the largest holes in the sample have a size of $\Delta\theta$, then the multipole decomposition becomes problematic around $\ell \sim 180°/\Delta\theta$. For the present sample this corresponds to $\ell \sim 2.5$, so that the quadrupole can be robustly fitted, but not the octupole. We have tested this in practice. When the quadrupole is added, the monopole and dipole amplitudes and the dipole direction hardly change. However, when the octupole is included there is serious leakage of power from the lower ℓ's to $\ell = 3$ and the results change substantially. The reason is that the fit in the well-sampled regions can be improved by adding the additional seven coefficients a_{3m} to the fit, but this happens at the expense of very large changes in the unsampled regions. In order to probe the higher order multipoles, it is essential to reduce the size of the

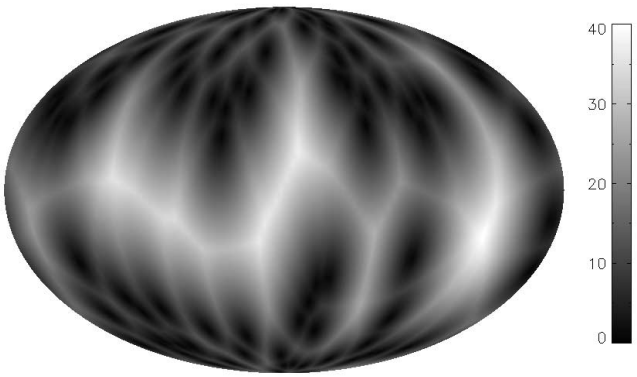

FIG. 5.—Shortest distance on the sky to a supernova (in degrees) using the "Hubble flow" sample. [*See the electronic edition of the Journal for a color version of this figure.*]

voids in the sample. For a uniformly distributed sample of 95 supernovae, the average distance to the nearest supernova is 10.4°, nearly the same as in the JRK sample. However, the average maximum distance is 30.1°, significantly lower than in our sample. A uniform sample of 95 supernovae could be used to probe $\ell = 3$ robustly. For a uniform sample, the average distance to the nearest supernova scales as $N^{-1/2}$, and the average maximum distance in the sample roughly as $N^{-0.4}$.

5.2. *Results*

On top of a map of the local universe (see Fig. 6 for coordinates and indications of superstructures), Figures 7–9 show the obtained 68% and 95% contours for the direction of the dipole and quadrupole vectors in Galactic coordinates. The corresponding best-fit values with their formal 68% errors are shown in Tables 1 and 2 and Figures 10–12. This result can be compared with other velocity surveys based on galaxy samples. The recent review by Sarkar et al. (2007) summarizes these surveys. At an effective depth of 4000 km s^{-1}, they find that the dipole amplitude is 330 ± 101 km s^{-1} in the direction $l = 234° \pm 11°$, $b = 12° \pm 9°$.

5.2.1. *Dipole*

The 3500 and 4500 samples both show a dipole in a direction compatible with the Great Attractor region at $(l, b) \sim (300°, 0°)$. For the HF sample, the direction shifts to slightly higher b, compatible with a shift in the motion toward the Shapley Concentration (which lies at an average distance of 14,000 km s^{-1}; Bardelli et al. 1994) at slightly higher Galactic latitude. Furthermore, the amplitude of the dipole decreases, as is expected from the Monte Carlo simulations.

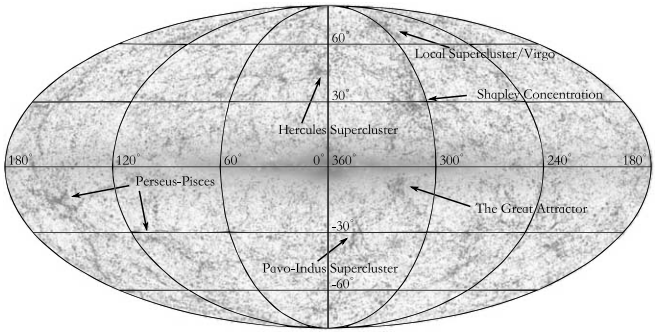

FIG. 6.—The local universe as seen by 2MASS. The galaxy distribution image is courtesy of T. H. Jarrett (IPAC/Caltech) and the 2MASS team. The complete image can be found at: http://spider.ipac.caltech.edu/staff/jarrett/papers/LSS. The arrows indicate important superclusters. [*See the electronic edition of the Journal for a color version of this figure.*]

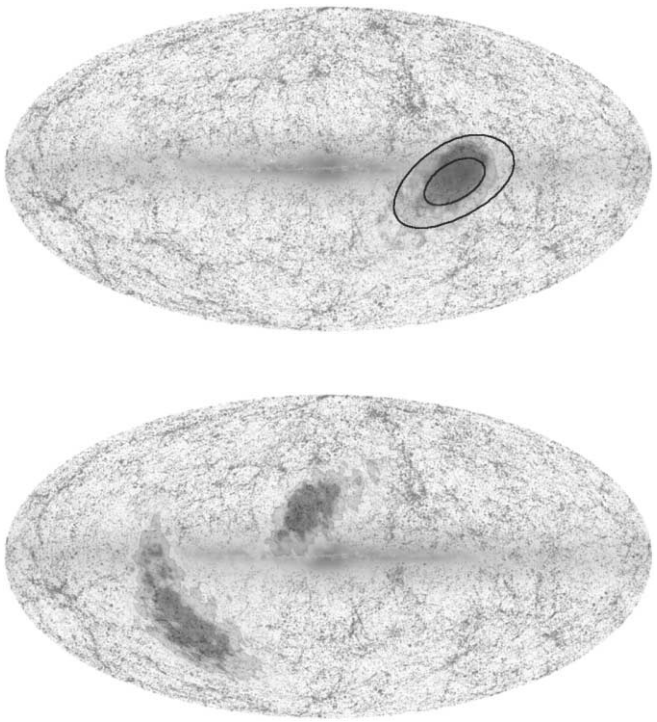

FIG. 7.—Dipole vector (*top*) and polar quadrupole vector (*bottom*) calculated from supernova data with a weighted average velocity of 3500 km s^{-1}. The ellipses show the 1 and 2 σ errors. [*See the electronic edition of the Journal for a color version of this figure.*]

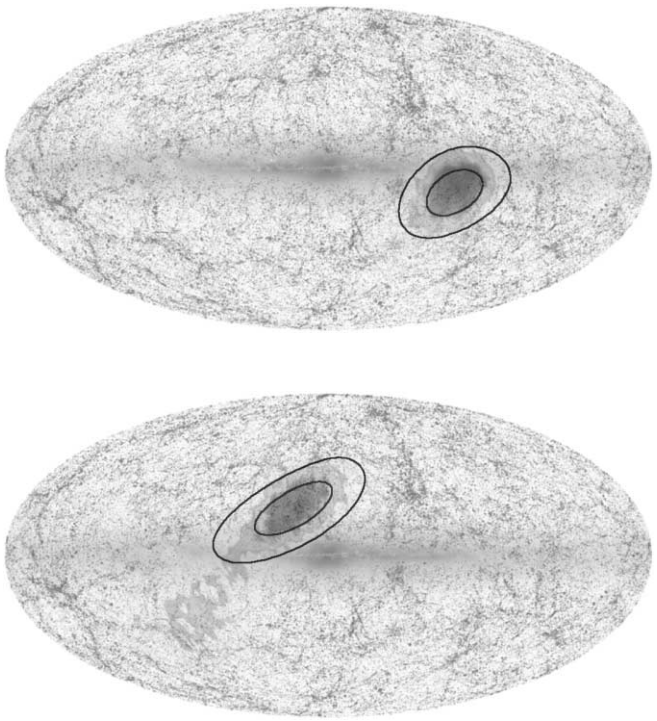

FIG. 8.—Same as Fig. 7, but calculated from SN Ia data with a weighted average velocity of 4500 km s^{-1}. [*See the electronic edition of the Journal for a color version of this figure.*]

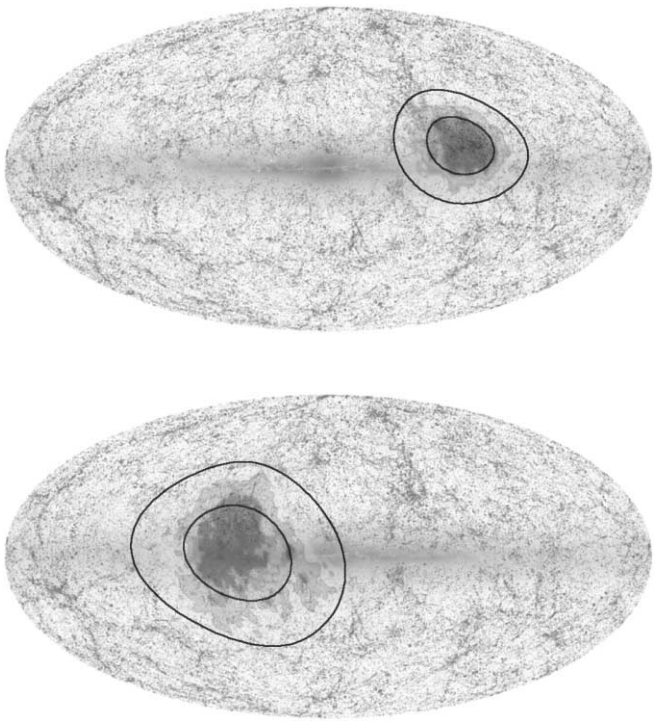

FIG. 9.—Same as Fig. 7, but calculated from the JRK "Hubble flow" sample. [*See the electronic edition of the Journal for a color version of this figure.*]

5.2.2. *Quadrupole*

For all three subsamples we find a relatively large contribution from the quadrupole, showing that the local flow has a significant shear component. This result is consistent in magnitude with the expectation from the Monte Carlo simulations. From the figures it can also be seen that there is a change in quadrupole direction with redshift, and that the distributions for the 3500 and 4500 samples are bimodal. This could be because the quadrupole is pointing in different directions at the lower and higher ends of the included redshift range of the SNe, and hence for the 3500 sample the bimodality would be more apparent. Even though we quote formal 68% errors in Table 2, the distribution is highly non-Gaussian (see Figs. 10 and 12) and the error bars should be taken as indicative only.

6. COMPARISON WITH OTHER RESULTS

6.1. *SNe Ia*

The Tonry et al. (2003) data set of 98 SNe was analyzed by Hudson et al. (2004) in order to find the local dipole. For the part of the sample with $v_r < 6000$ km s^{-1}, they found a dipole of $v_r = 376 \pm 81$ km s^{-1} toward $l = 285^\circ$, $b = -14^\circ$. They do not quote error bars on this result, but for the part of the sample with $v_r > 6000$ km s^{-1}, the stated errors are $\pm 17^\circ$ for l and

TABLE 1

AMPLITUDE AND DIRECTION OF THE DIPOLE VECTOR FOR THE THREE SAMPLES

Sample	v_r (km s^{-1})	l (deg)	b (deg)
3500.....	280^{+67}_{-88}	289^{+23}_{-25}	-11^{+24}_{-17}
4500.....	279^{+57}_{-79}	285^{+15}_{-20}	-10^{+15}_{-14}
HF	239^{+70}_{-96}	281^{+21}_{-24}	14^{+16}_{-15}

TABLE 2

AMPLITUDE OF THE QUADRUPOLE AND DIRECTION OF THE POLAR QUADRUPOLE VECTOR FOR THE THREE SAMPLES

Sample	v_r (km s^{-1})	l (deg)	b (deg)
3500.....	654^{+129}_{-144}	68^{+49}_{-55}	-5^{+45}_{-36}
4500.....	575^{+116}_{-137}	43^{+46}_{-44}	10^{+36}_{-34}
HF	522^{+127}_{-159}	56^{+35}_{-41}	3^{+30}_{-28}

$\pm 13^\circ$ for b. This result is completely compatible with our result for the dipole. However, Hudson et al. quote no results for the higher order terms.

Jha et al. (2007) also provide a crude estimate of the dipole amplitude and direction from a subset of 69 supernovae in their sample that is roughly compatible with our 4500 sample. In the coordinate system of the Local Group, they find a velocity of 541 ± 75 km s^{-1} toward a direction of $l = 258^\circ \pm 18^\circ$, $b = 51^\circ \pm 12^\circ$. If we transform our dipole term from the HF sample to the same coordinate system, using the Local Group velocity derived by Rauzy & Gurzadyan (1998), we find a velocity of 516 km s^{-1} toward $(l, b) = (248^\circ, 51^\circ)$. Both the amplitude and direction are compatible with the JRK value at 1 σ. Our derived amplitude is slightly lower (although not significantly so), because in our fit the quadrupole term accounts for part of the velocity.

As noted above, we do not discuss the local monopole term. By subdividing supernovae into low- and high-redshift bins (Zehavi et al. 1998; Jha et al. 2007), a significant variation in the local Hubble parameter has been detected. This does not have any impact on our results (see § 5.1), and since it was discussed

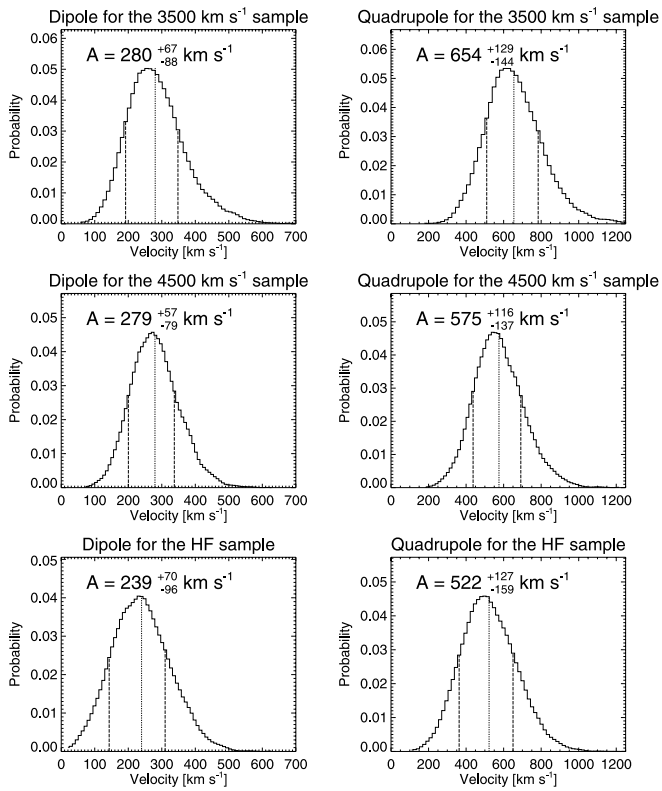

FIG. 10.—One-dimensional distributions of velocity amplitude for the different samples, with 68% limits indicated by dashed lines and the median value by a dotted line.

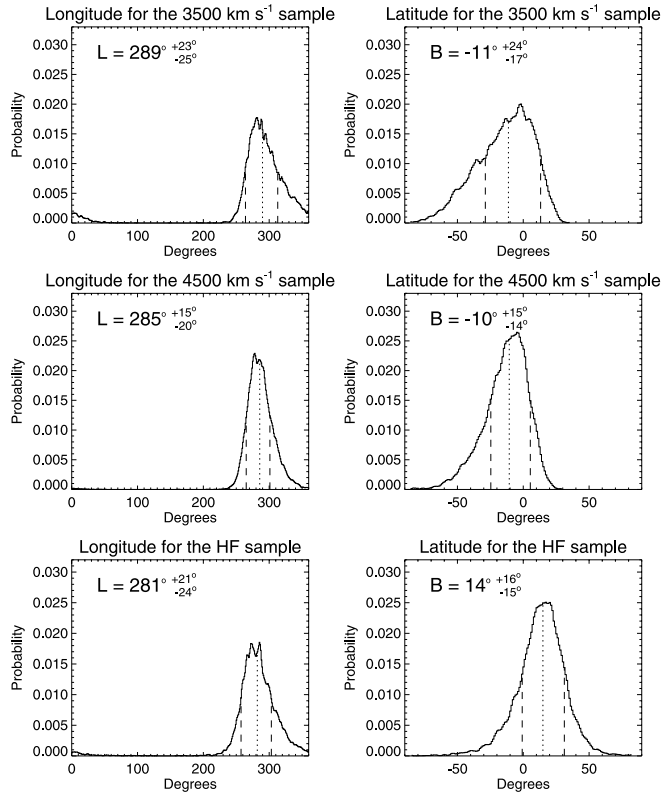

FIG. 11.—Same as Fig. 10, but for the dipole vectors.

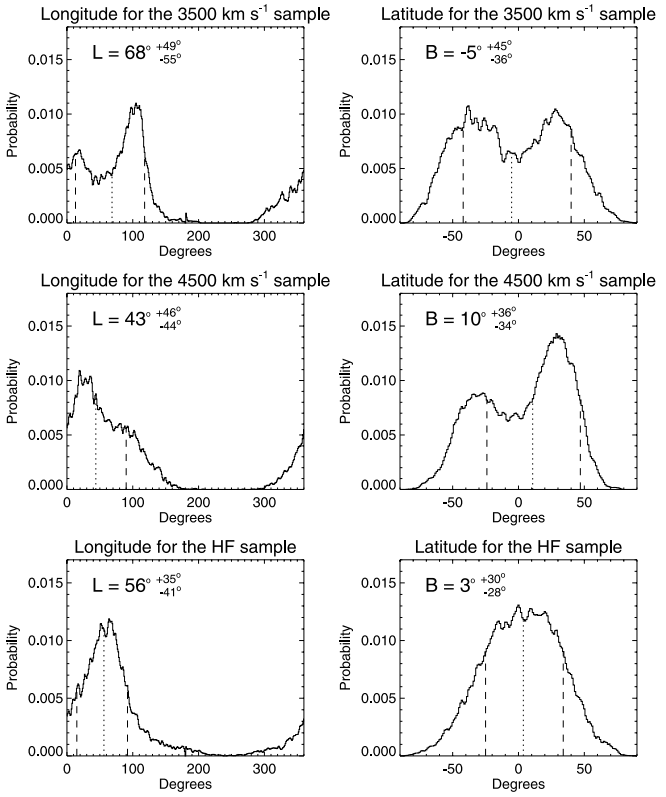

FIG. 12.—Same as Fig. 10, but for the polar quadrupole vectors.

thoroughly in Jha et al. (2007), we refer the reader to that paper for further details.

6.2. *Galaxy Surveys*

Results from galaxy velocity surveys on scales of ∼4000–6000 km s^{-1} generally agree that the magnitude of the dipole is on the order of 300 km s^{-1} in the direction $(l, b) \sim (300^\circ, 20^\circ)$ (see, e.g., Zaroubi 2004 and references therein). This result is compatible with the SN Ia dipole direction and magnitude within 2 σ.

A reconstruction of the very local velocity field (<3000 km s^{-1}) was done by Tonry et al. (2000) by measuring surface brightness fluctuations in 300 early-type galaxies, predominantly in groups and clusters. They used an explicit flow model with a Virgo Attractor and a Great Attractor, which contain the main local mass concentrations. Furthermore, they added dipole and quadrupole terms to account for the gravitational pull and shear from large-scale structure farther away. They find a very low value for the dipole (∼150 km s^{-1}) and the quadrupole polar vector (∼50 km s^{-1}), but this may be related to having the dipole in the same direction as the attractors, and the attractors' accounting for the major part of the shear (quadrupole term) in the model.

The dipole has also been measured using velocity field reconstruction from the density field of galaxies. Using the Two Micron All Sky Survey (2MASS) catalog, at a distance of 4000–6000 km s^{-1} the dipole direction is found to be roughly $l \sim 250^\circ$, $b \sim 35^\circ - 40^\circ$, again compatible with our result within 2 σ (Erdoğdu et al. 2006a, 2006b; Pike & Hudson 2005). Radburn-Smith et al. (2004) compared the reconstructed velocity field from the PSC*z* catalog (Saunders et al. 2000) with peculiar velocities of 98 SNe Ia to constrain the gas–to–dark matter density contrast. They find excellent agreement between the two data sets, and a dipole of 206 ± 97 km s^{-1} toward $l = 290^\circ \pm 25^\circ$, $b = 0^\circ \pm 18^\circ$.

6.3. *Clusters*

Cluster samples such as SMAC (Streaming Motions of Abell Clusters) probe larger distances and find directions that are generally compatible with the SN Ia result. For example, Hudson et al. (2004) find $l = 260^\circ \pm 13^\circ$, $b = 0^\circ \pm 11^\circ$. However, they find an amplitude of 687 ± 203 km s^{-1}, significantly higher than our result (although again compatible at 2 σ).

7. DISCUSSION

We have analyzed mock supernova surveys in order to study the number of supernovae needed to probe the large-scale velocity field of the local universe, quantified in terms of the angular power spectra as a function of redshift. We then proceeded to use the best available database of low-redshift supernovae, the JRK sample, to probe the local dipole and quadrupole of the velocity field at three different distances. The present method has several advantages over galaxy surveys. The uncertainty on each individual supernova luminosity is much smaller than the systematic uncertainties in determining galaxy luminosities, so that a much smaller sample is sufficient. We find the following:

1. With two different models for the Type Ia supernova rate, the resulting mock surveys only differ at the few-percent level. Hence, using SNe Ia to probe the underlying velocity field is robust with respect to assumptions about the supernova environment.

2. For the dipole, we find a result that is consistent with galaxy surveys at the same Hubble flow depths.

3. The quadrupole is comparable in value to the dipole, indicative of a significant shear in the local velocity field, in accordance with our mock catalogs. It has, to our knowledge, not been measured before at these distances.

4. With the present sample size of almost 100 supernovae, the precision of the dipole measurement is comparable to that in galaxy surveys using thousands of galaxies.

Finally, we note that new surveys such as Pan-STARRS, SkyMapper, and LSST will measure about 10,000 Type Ia supernovae at $z < 0.1$ per year, and if proper light curves and redshifts can be measured for even a small fraction of these events, they will provide an extremely powerful tool for studying the dynamics of the local universe.

We thank the Danish Centre of Scientific Computing for granting the computer resources used. T. H. thanks the Dark Cosmology Centre for hospitality during the course of this work. S. J. is grateful for support at KIPAC and SLAC through the Panofsky Fellowship. The Dark Cosmology Centre is funded by the Danish National Research Foundation.

REFERENCES

Aldering, G., et al. 2002, Proc. SPIE, 4836, 61
Bardelli, S., Zucca, E., Vettolani, G., Zamorani, G., Scaramella, R., Collins, C. A., & MacGillivray, H. T. 1994, MNRAS, 267, 665
Bonvin, C., Durrer, R., & Gasparini, M. A. 2006a, Phys. Rev. D, 73, No. 023523
Bonvin, C., Durrer, R., & Kunz, M. 2006b, Phys. Rev. Lett., 96, No. 191302
Copi, C. J., Huterer, D., Schwarz, D. J., & Starkman, G. D. 2006, MNRAS, 367, 79
Erdoğdu, P., et al. 2006a, MNRAS, 368, 1515
———. 2006b, MNRAS, 373, 45
Frieman, J., et al. 2004, BAAS, 36, 1548
Hamuy, M., et al. 2006, PASP, 118, 2
Hudson, M. J., Smith, R. J., Lucey, J. R., & Branchini, E. 2004, MNRAS, 352, 61
Hui, L., & Greene, P. B. 2006, Phys. Rev. D, 73, No. 123526
Jha, S., Riess, A. G., & Kirshner, R. P. 2007, ApJ, 659, 122
Jha, S., et al. 2006, AJ, 131, 527
Karachentsev, I. D., et al. 2003, A&A, 398, 479
Krisciunas, K., et al. 2004, AJ, 128, 3034 (erratum 130, 350 [2005])
Li, W., et al. 2003, PASP, 115, 453
Miller, D. L., & Branch, D. 1992, AJ, 103, 379
Neill, J. D., et al. 2006, AJ, 132, 1126
Pike, R. W., & Hudson, M. J. 2005, ApJ, 635, 11
Radburn-Smith, D. J., Lucey, J. R., & Hudson, M. J. 2004, MNRAS, 355, 1378
Rauzy, S., & Gurzadyan, V. G. 1998, MNRAS, 298, 114
Riess, A. G., Press, W. H., & Kirshner, R. P. 1995, ApJ, 445, L91
Riess, A. G., et al. 2004, ApJ, 607, 665
Sarkar, D., Feldman, H. A., & Watkins, R. 2007, MNRAS, 375, 691
Saunders, W., et al. 2000, MNRAS, 317, 55
Sharon, K., Gal-Yam, A., Maoz, D., Filippenko, A. V., & Guhathakurta, P. 2007, ApJ, 660, 1165
Springel, V. 2005, MNRAS, 364, 1105
Springel, V., Yoshida, N., & White, S. D. M. 2001, NewA, 6, 79
Sugiura, N., Sugiyama, N., & Sasaki, M. 1999, Prog. Theor. Phys., 101, 903
Sullivan, M., et al. 2006, ApJ, 648, 868
Tonry, J. L., Blakeslee, J. P., Ajhar, E. A., & Dressler, A. 2000, ApJ, 530, 625
Tonry, J. L., et al. 2003, ApJ, 594, 1
Zaroubi, S. 2004, in Frontiers of the Universe, ed. L. Celnikier & J. Trân Thanh Vân (Hanoi: Thê Giói), 65
Zehavi, I., Riess, A. G., Kirshner, R. P., & Dekel, A. 1998, ApJ, 503, 483